



HAL
open science

Next Generation SiGe HBTs for Energy Efficient Microwave Power Amplification (Invited)

Soumya Ranjan Panda, Philippine Billy, Alexis Gauthier, Nicolas Guitard,
Pascal Chevalier, Magali De Matos, Thomas Zimmer, Sebastien Fregonese

► **To cite this version:**

Soumya Ranjan Panda, Philippine Billy, Alexis Gauthier, Nicolas Guitard, Pascal Chevalier, et al..
Next Generation SiGe HBTs for Energy Efficient Microwave Power Amplification (Invited). 2024
8th IEEE Electron Devices Technology & Manufacturing Conference (EDTM), Mar 2024, Bangalore,
India. pp.1-3, 10.1109/EDTM58488.2024.10511770 . hal-04603010

HAL Id: hal-04603010

<https://hal.science/hal-04603010v1>

Submitted on 6 Jun 2024

HAL is a multi-disciplinary open access archive for the deposit and dissemination of scientific research documents, whether they are published or not. The documents may come from teaching and research institutions in France or abroad, or from public or private research centers.

L'archive ouverte pluridisciplinaire **HAL**, est destinée au dépôt et à la diffusion de documents scientifiques de niveau recherche, publiés ou non, émanant des établissements d'enseignement et de recherche français ou étrangers, des laboratoires publics ou privés.

Next Generation SiGe HBTs for Energy Efficient Microwave Power Amplification (Invited)

Soumya Ranjan Panda¹, Philippine Billy^{1,2}, Alexis Gauthier², Nicolas Guitard², Pascal Chevalier²
Magali De Matos¹, Thomas Zimmer¹, and Sebastien Fregonese¹

¹IMS Laboratory, University of Bordeaux, Talence, 33400, France, email: soumya-ranjan.panda@u-bordeaux.fr

²STMicroelectronics, 38920 Crolles, France

Abstract— The linearity and efficiency of two distinct SiGe HBT devices, manufactured using different process technologies (B55 & B55X prototype) by STMicroelectronics, are examined with a focus on energy-efficient applications under large-signal conditions.

Keywords: SiGe HBT, Load pull, Microwave Power Amplifier Efficiency

I. INTRODUCTION

Silicon Germanium (SiGe) heterojunction transistors have been demonstrated as a viable substitute for III-V devices owing to their cost-effectiveness, and superior radio frequency (RF) performance compared to CMOS devices. As wireless communication frequencies advance into the millimeter wavelength range (mmW), SiGe BiCMOS devices also find application in the design of power amplifiers within the sub-6 GHz frequency range. The advent of modern communication standards, such as 802.11 Wi-Fi and 4G/6G wireless communication, necessitates the design of highly efficient radio frequency power amplifiers (RFPA) to accommodate the substantial peak-to-peak average power ratio of RF signals. Commencing with linearity and efficiency, these are pivotal figures of merit (FoMs) for high-frequency Power Amplifiers (PAs). In applications such as wireless communication, devices characterized by high linearity can mitigate signal distortion, while those with high efficiency can extend battery life [1].

Next generation SiGe BiCMOS HBT have demonstrated enhancements in cutoff and oscillation frequency (f_T , f_{MAX}) achieved at the cost of open base collector (BV_{CEO}) which is consistently diminishing. In device model cards and Process Design Kits (PDKs), BV_{CEO} is commonly specified as the upper usable limit of V_{CE} , representing the transistor's dynamic voltage swings [2]. The advent of large-signal characterization setups, capable of characterizing time-domain waveforms of both voltage and current at the transistor reference plane, facilitates optimization of both device technology and circuit. These setups can determine the maximum voltage and/or current amplifiers at the input and output port of the device under test (DUT), crucial for both device reliability and PA design. While maximum swing is correlated with the absolute maximum ratings of the transistor, it has been demonstrated that bipolar devices can operate well beyond these ratings. This work aims to demonstrate that, in RF dynamic operation, instantaneous voltage and current at the output terminal (i.e., collector in

the common-emitter configuration) represented as $v_c(t)$ & $i_c(t)$ swings can transiently traverse regions in the output characteristics unreachable during DC operation.

Moreover, the advancement of SiGe Heterojunction Bipolar Transistor (HBT) devices within the B55X prototype process line at STMicroelectronics demonstrates enhanced RF and self-heating performance at a reduced cost. The large-signal performance of this device is juxtaposed with the well-established SiGe HBT device manufactured in the B55 process line. This study elucidates the impact of the aforementioned factors and draws comparisons between STMicroelectronics' B55 and B55X technologies in the context of large-signal power amplifier operation, employing load-pull characterization at a fundamental frequency of 3 GHz. The performance enhancements in the B55X technology for energy-efficient applications are compared.

II. LOAD-PULL MEASUREMENTS

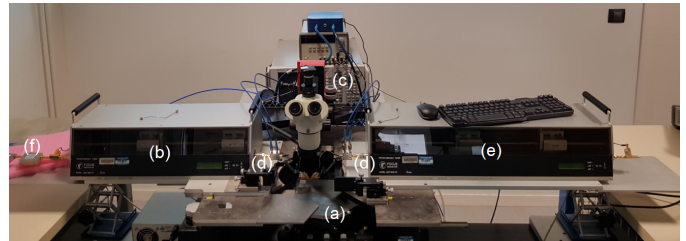


Fig. 1: Vectored load-pull measurement setup depicting different sections like (a) DUT, (b/e) source-load tuners, (c) VNA, (d) coupler, (f) power source.

Load-pull measurements provide insights into how a device can deliver power (P_{out}) and efficiency (PAE) to a load under different impedance conditions at high frequencies. The load-pull measurement setup is depicted in Fig.1 is employed to characterize both DC aspects and large-signal RF behaviors. In this vectored load-pull measurement setup the forward (a_1 , b_1) and reverse (a_2 , b_2) traveling waves are measured using the two directional couplers connected at the input and output port of the DUT. Measuring a and b waves forms allows vector load-pull to calculate the real time tuner impedance presented to the DUT and does not fully rely on tuner calibration and repeatability.

In this study, only load tuners are utilized, where the optimal load impedance is achieved based on stimulus monitored by stepper motors and tuner controllers. The reference plane during characterization is adjusted, along with bias-tees calculated from small-signal S -parameter measurements. A Continuous Wave (CW) RF signal, generated by the signal generator, drives the SiGe Heterojunction Bipolar Transistor (HBT) device under test (DUT). The output signal power is measured up to the 3rd harmonics ($3\times$ fundamental frequency (f_0 , 3 GHz).

III. B55 HICUM MODEL CARD VERIFICATION

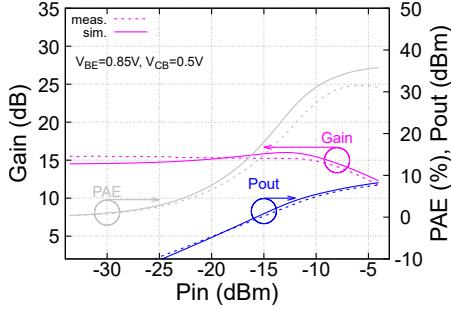


Fig. 2: P_{out} , G & PAE vs. P_{in} measurement (dashed lines) and simulated (solid lines) measured at source (Z_S) and load (Z_L) impedance of $50\ \Omega$ impedance at different input and DC bias of $V_{BE}=0.85\text{ V}$, and $V_{CE}=1.35\text{ V}$, $f_0 = 3\text{ GHz}$.

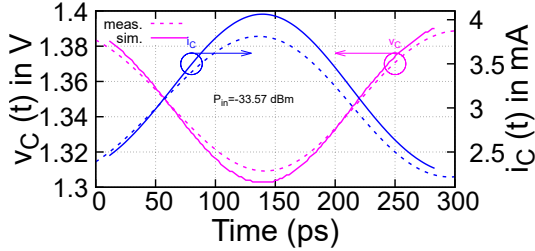


Fig. 3: Measured and simulated collector current and voltage wave forms plotted w.r.t time at $V_{BE}=0.85\text{ V}$, and $V_{CE}=1.35\text{ V}$, $f_0 = 3\text{ GHz}$.

To ascertain the maximum linear output power (P_{out}), Gain (G), and Power Added Efficiency (PAE) of the unmatched B55 SiGe HBT device [3], AM/AM characteristics are measured. The measurements are conducted with both input and output impedances fixed at $50\ \Omega$ at a fundamental frequency of 3 GHz, and unless explicitly mentioned, it is biased at $V_{BE}=0.85\text{V}$ and $V_{CE}=1.35\text{V}$. The input power (P_{in}) is swept from -33 dBm to -3 dBm to encompass both the linear and compression regions. The resulting P_{out} , Gain, and PAE are depicted in Fig.2.

Similarly, the measured time-domain waveforms (cf. Fig.3, $v_c(t)$ & $i_c(t)$) at a fixed P_{in} of -33.57 dBm) are computed from the values of traveling waves spectral components at the DUT reference plane. To scrutinize the impact of self-heating the measured characteristics shown in Fig.2&3 are reproduced using Harmonic-Balance simulation, considering

the B55 device model card [4]. The results validate a high level of concordance between the measurements and simulations. The output characteristics has been simulated at V_{BE} up to 1.1 V, and V_{CE} up to 2.6 V switching the thermal resistance (R_{TH}) in the model-card on and off. The output loadlines (v_c , i_c) were extracted at two different input power -14.8 dBm ($\sim 1\text{ dB}$ compression point) and at a possible very high P_{in} of -3.73 dBm at discussed R_{TH} condition. The impact of R_{TH} on the output characteristics (see Fig. 4) is clearly visible and we can also observe from the loadlines that it has less impact on the large signal operation. This confirms the device can operate effectively well above the DC range ($V_{BE}=0.9\text{V}$, $V_{CE}=1.5\text{V}$) within the microwave frequency range. The same is depicted by plotting the time domain sinusoidal waveforms in Fig.5.

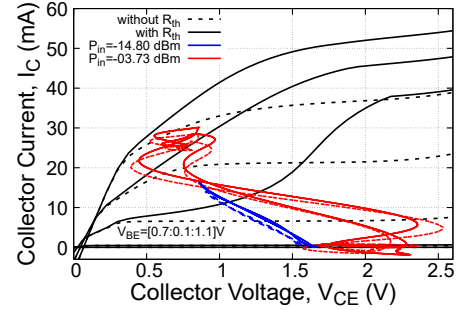


Fig. 4: Simulation of loadlines at $V_{BE}=0.85\text{V}$, $V_{CE}=1.35\text{V}$ superimposed on DC output characteristics to observe impact of self-heating (R_{TH}) beyond normal operating range.

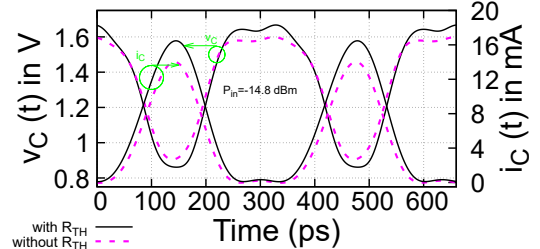


Fig. 5: Simulation of time-domain waveforms at $V_{BE}=0.85\text{V}$, $V_{CE}=1.35\text{V}$ to observe impact of self-heating (R_{TH}). Here reference (with R_{TH}) stands for the B55 standard available model card without any modifications in R_{TH} parameter value.

IV. B55X DEVICE TECHNOLOGY & FOM COMPARISON WITH B55

The matured B55 and the proposed B55X SiGe HBTs are fabricated at STMicroelectronics using 55 nm BiCMOS technology. In the B55X, the major modifications involve the adoption of the extrinsic base isolated from the collector (EXBIC) architecture [5]. These modifications include: (i) replacing the buried layer with a shallow implanted collector, (ii) utilizing phosphorous and carbon co-implantation to achieve the targeted f_T/BV_{CBO} trade-off, and (iii) employing super

shallow trench isolation (SSTI) for isolation between the extrinsic parts of the base and the collector. This is made possible by shallow doping profiles, and external isolation is achieved using Shallow Trench Isolation (STIs) instead of Deep Trench Isolation (DTIs), resulting in approximately 10% cost savings in production compared to the corresponding B55 technology [5]. Furthermore, the absence of DTIs leads to a significant reduction in self-heating. A comparison of the performance improvements is presented in Table.I.

TABLE I: Comparison of B55, B55X FoMs.

	B55 [3]	B55X [5]	B55X Prototype
f_T (GHz)	320	390 at $V_{CB}=0.3V$	340 at $V_{CB}=0V$
f_{MAX} (GHz)	370	500 at $V_{CB}=0.3V$	480 at $V_{CB}=0V$
BV_{CEO} (V)	1.5	1.45	1.45

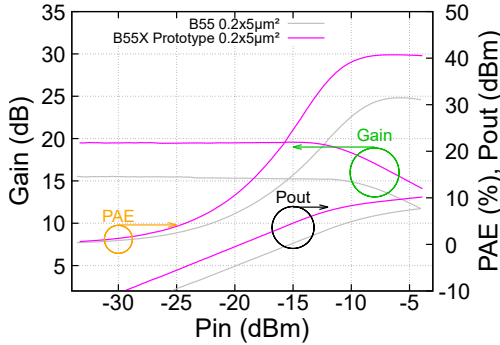


Fig. 6: P_{out} , G , PAE vs. P_{in} for both B55 and B55X devices having same dimension, measured at DC bias of $V_{BE}=0.85$ V, and $V_{CE}=1.35$ V, $f_0 = 3$ GHz, at $Z_{S,L}$ of 50Ω .

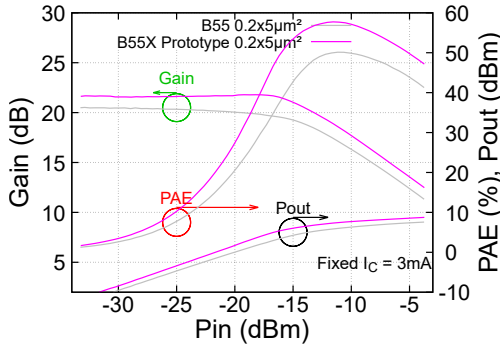


Fig. 7: P_{out} , G , PAE vs. P_{in} for both B55 and B55X devices having same dimension, measured at DC bias of $V_{BE}=0.85$ V for B55, 0.8326 V for B55X (to have same collector current of $\simeq 3$ mA) and $V_{CE}=1.35V$, frequency = 3 GHz, Z_S 50Ω & optimized Z_L .

From the AM/AM characteristics depicted in Fig.6, it is evident that the B55X device exhibits higher P_{out} ($\sim 28\%$) and efficiency ($\sim 26\%$) in comparison to its B55 counterpart. However, as the devices are measured under unoptimized load

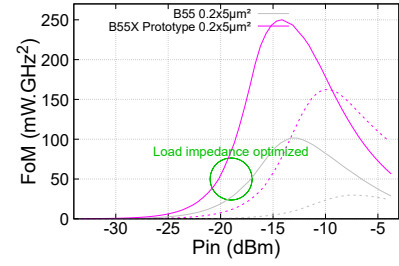


Fig. 8: ITRS power performance FoM calculated at measurement conditions mentioned in Fig.6 (dashed lines) & 7 (solid lines).

conditions, the overall efficiency is lower. Additionally, since the DC bias conditions are identical for both devices, a fair comparison between the technologies and their respective improvements cannot be established. To ensure a fair comparison between B55 and B55X devices, the load impedance is matched for both devices, maintaining V_{CE} at 1.35 V. The V_{BE} for the B55X device is adjusted to ensure that the collector current falls within the same range as B55 (i.e., $I_C = 3$ mA).

To quantitatively assess the improvement in power performance, the International Technology Roadmap for Semiconductors (ITRS) Figure of Merit (FoM) is employed, defined as $FoM = P_{out} \cdot G \cdot PAE \cdot f^2$ (mW.GHz), considering all three individual FoMs: P_{out} , G , and PAE [6]. As illustrated in Fig.8, a significant improvement ($\sim 85\%$) in ITRS FoM is observed in B55X when measured under optimized load impedance, compared to B55 measured under same measurement conditions.

V. CONCLUSION

The large-signal characteristics of a SiGe HBT-based microwave power amplifier were investigated, and the amplification and efficiency were compared with respect to process modifications. The SiGe HBT being developed in the B55X process line exhibits superior large-signal performance, making it advantageous for energy-efficient applications in microwave power amplifiers.

ACKNOWLEDGMENT

We would like to thank SHIFT project (ID-101096256), FRANCE 2030 and BPIFRANCE for the financial support and STMicroelectronics for the Silicon wafers.

REFERENCES

- [1] Osrecki *et al.*, "Measurement of RF linear Operating Area of Bipolar Transistors." IEEE Microwave and Wireless Components Letters, 2020.
- [2] Weimer *et al.*, "An Experimental Load-Pull Based Large-Signal RF Reliability Study of SiGe HBTs", IEEE BCICTS, 2021.
- [3] Chevalier *et al.*, "A 55 nm Triple Gate Oxide 9 Metal Layers SiGe BiCMOS Technology Featuring 320 GHz f_T / 370 GHz f_{MAX} HBT and High-Q Millimeter-Wave Passives", IEDM 2014.
- [4] Panda *et al.*, "Exploring compact modeling of SiGe HBTs in Sub-THz range with HICUM", IEEE TED, 2023.
- [5] Gauthier *et al.*, "Low-noise Si/SiGe HBT for LEO satellite user terminals in Ku-Ka bands", IEEE BCICTS 2023.
- [6] Ma *et al.*, "Base-Region Optimization of SiGe HBTs for High-Frequency Microwave Power Amplification." IEEE TED, 2006.